J Appl Electrochem (2009) 39:751–759
DOI 10.1007/s10800-008-9719-8

ORIGINAL PAPER

# Effect of nickel sulphate and magnesium sulphate on pH of sulphuric acid solutions at elevated temperatures

**Z. Jankovic · V. G. Papangelakis · S. N. Lvov**

**Abstract** A flow-through potentiometric technique utilizing an yttria-stabilized zirconia (YSZ) pH sensor has been employed to elucidate the effects of $NiSO_4$ and $MgSO_4$ on pH of $H_2SO_4$ solutions at temperatures of 200 °C and 250 °C. Solution pH was found to increase with increasing $NiSO_4$ and $MgSO_4$ concentrations at both temperatures. This trend is attributed to the dissociation of $NiSO_4$ and $MgSO_4$ where the $SO_4^{2-}$(aq) released reacts with $H^+$(aq) to form $HSO_4^-$(aq). The conversion of measured potentials into pH values was based on the mixed-solvent electrolyte (MSE) model, which is a speciation model of the new OLI Systems® software. Both the Henderson equation and exact definition of the diffusion potential were employed in treating the obtained experimental data. Experimental pH values calculated using the diffusion potentials evaluated by either approach are similar, suggesting that the Henderson equation can be effectively used. In addition, LiCl was found to be a suitable alternative to NaCl as the reference electrode solution.

**Keywords** High-temperature pH measurement · Yttria-stabilized zirconia sensor

Z. Jankovic · V. G. Papangelakis (✉)
Department of Chemical Engineering and Applied Chemistry,
University of Toronto, 200 College Street,
Toronto, ON, Canada M5S 3E5
e-mail: vladimiros.papangelakis@utoronto.ca

S. N. Lvov
Department of Energy and Mineral Engineering,
The Pennsylvania State University, University Park,
PA 16802-2714, USA
e-mail: lvov@psu.edu

## 1 Introduction

Many industrial installations are processing concentrated electrolyte solutions at elevated temperatures. A typical case is the pressure acid leach (PAL) process for Ni and Co recovery from laterite ores, which takes place at around 250 °C [1, 2]. Depending on the ore composition, the leach solution exiting from the autoclave contains concentrated $H_2SO_4$ at 0.20–0.50 mol $kg^{-1}$, as well as dissolved metal sulphates of Ni, Co, Mg, Mn, Al and Fe. The Ni, Mg, Mn and Al concentrations in the leach solution range from 0.05 to 0.5 mol $kg^{-1}$, the Co concentration is about 0.01 mol $kg^{-1}$, and the concentration of Fe is less then 0.01 mol $kg^{-1}$ [1, 2]. In the leaching process, the extraction of Ni and Co from laterite ores to the aqueous solution is an acid-driven process [3]. Therefore, to control the extent of dissolution reactions, it is important to know the solution chemistry and, in particular, the solution pH.

In our initial experiments using a flow-through yttria-stabilized zirconia (YSZ) electrode, pH was measured in binary $H_2SO_4$–$H_2O$, ternary $Al_2(SO_4)_3$–$H_2SO_4$–$H_2O$ and quaternary $MgSO_4$–$Al_2(SO_4)_3$–$H_2SO_4$–$H_2O$ systems at 250 °C [4]. Aluminium sulphate was found to have insignificant effect on pH. On the other hand, increasing $MgSO_4$ concentration resulted in an increase of pH corresponding to a decrease of $H^+$(aq) activity. This phenomenon was attributed to the dissociation of $MgSO_4$, with the extra $SO_4^{2-}$(aq) released readily reacting with $H^+$(aq) to form $HSO_4^-$(aq) [5]. However, Al is known to associate with its own $SO_4^{2-}$(aq) in acidic sulphate solutions [5–7]. Hence, most of the aluminium was complexed, such that the loss of $H^+$(aq) to $HSO_4^-$(aq) formation was much lower, resulting in negligible pH dependence. The conversion of measured potentials into pH values was based on an extended Debye-Hückel approximation, whereas the OLI Systems® software was based on the Bromley-Zemaitis activity equation. An explicit integration was employed for calculating diffusion potentials between acidic solutions and the 0.1 mol kg$^{-1}$ NaCl reference electrode solution. The method of converting the measured potentials to pH has been published previously [8].

Our previous work [4] aimed at confirming whether this method as well as the YSZ electrode would work under concentrated acidic environments, such as those encountered in industry. After these initial confirmatory experiments, the pH of PAL solutions was measured [9]. During these measurements, scale formation at the outlet of the electrochemical cell was observed. The scale was produced because of the mixing of the aluminium-containing PAL solutions and the NaCl reference electrode solution. This observation was consistent with the fact that sodium alunite, $NaAl_3(SO_4)_2(OH)_6$, is less soluble than hydronium alunite, $H_3OAl_3(SO_4)_2(OH)_6$ [2].

Thus, the purpose of the present work is several-fold. First, we are interested to investigate the effect of $NiSO_4$ on the pH of $H_2SO_4$ solutions because nickel is the most abundant metal in PAL solutions of low-magnesium laterite ores. Second, we want to also examine the effect of $MgSO_4$ on the pH of $H_2SO_4$ solutions because magnesium is the most abundant soluble impurity in certain types of laterites. Furthermore, it would be interesting to use the mixed-solvent electrolyte (MSE) model embedded in the new OLI Systems® software to convert the measured potentials into pH values and, by this way, to improve the accuracy of the conversion from the measured potential to pH. Also, one of our goals is to investigate whether the simple Henderson equation [10] provides an acceptable accuracy when used instead of the explicit integration for calculating the diffusion potential. Finally, we are interested to investigate whether the use of NaCl as the reference electrode solution can be replaced with another chloride electrolyte that will prevent the precipitation of Al and Fe compounds in the electrochemical cell.

## 2 Experimental

The configuration of the flow-through electrochemical cell used for potentiometric pH measurements is illustrated in Fig. 1 [4, 11]. The cell consists of a cylinder made of titanium Grade 5 into which a flow-through yttria-stabilized zirconia (YSZ) pH electrode [12, 13] and a flow-through external pressure-balanced Ag/AgCl reference electrode [13, 14] were sealed. The YSZ electrodes were made of a $ZrO_2$ (9 wt.% $Y_2O_3$) tube from CoorsTeck, Hg/HgO paste, and a Pt wire according to procedures published elsewhere [12]. Two YSZ electrodes were used. The first electrode, denoted YSZ-1, was used in experiments at 250 °C, while the second electrode, referred to as YSZ-2, was used in tests at 200 °C.

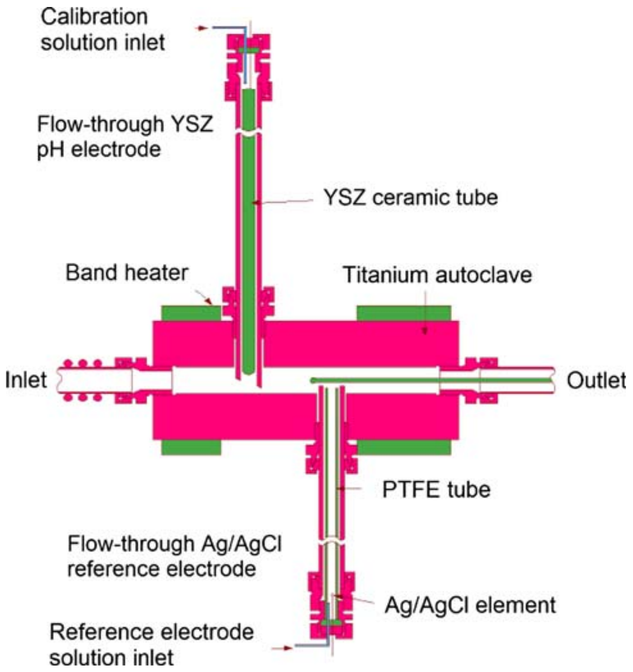

**Fig. 1** Schematic of the the flow-through electrochemical cell used for potentiometric pH measurements [4, 11]

Three high-pressure liquid chromatography pumps were employed to pump the solutions at a fixed flow rate of 0.5 mL min$^{-1}$. The reference solution (either 0.1 mol kg$^{-1}$ NaCl or 0.1 mol kg$^{-1}$ LiCl) was constantly pumped through the flow-through Ag/AgCl reference electrode. During the calibration, standard solutions were pumped through the flow-through YSZ electrode. After the calibration, pumping of the standard solutions was stopped and test solutions were pumped through the inlet of the cell. Measurements were performed at a constant pressure of 8 MPa. The potential difference between the YSZ electrode and the reference electrode was measured using a Keithley electrometer with an input impedance of $10^{14}$ Ω. Further experimental details are given elsewhere [4].

## 3 Theory

The yttria-stabilized zirconia electrode is considered a primary pH sensor [15] and may be used for measuring pH without prior calibration under conditions of thermodynamic equilibrium. When using a flow-through YSZ electrode, however, irreversible thermodynamics contributions should be taken into account [12, 13, 16]. As a result, a particular calibration procedure has been developed [4, 13]. This procedure involves measuring the potentials of at least two standard solutions, and evaluating the value of a calibration coefficient for the YSZ electrode, which takes into account deviation from the electrode behaviour under thermodynamic equilibrium. Once calibrated, the YSZ electrode can be used to measure a test solution potential.

The calculation of the calibration coefficient, α, is based on the following equation [4, 13]

$$\mathrm{pH}_1 - \mathrm{pH}_2 = -\alpha\frac{(E_1 - E_2)}{\frac{2.303RT}{F}} - \frac{1}{2}\log\left[\frac{a^{(1)}_{H_2O}}{a^{(2)}_{H_2O}}\right] + \frac{\left(\Delta\phi^{(1)}_D - \Delta\phi^{(2)}_D\right)}{\frac{2.303RT}{F}} \tag{1}$$

where $\mathrm{pH}_1$ and $\mathrm{pH}_2$ are the pH values of solutions 1 and 2; $E_1$ and $E_2$ are the measured potentials of the YSZ electrode versus the reference electrode; $\Delta\phi^{(1)}_D$ and $\Delta\phi^{(2)}_D$ are the diffusion potentials; and $a^{(1)}_{H_2O}$ and $a^{(2)}_{H_2O}$ are the activities of water for solutions 1 and 2, respectively. The potentials of the standard solutions are experimentally measured; the pH values and water activities are calculated from established and verified thermodynamic data, while the diffusion potentials have to be independently calculated. In the present work, pH values of the standard solutions and water activities were calculated with OLI Systems® software (Stream Analyzer, version 2.0.54, www.olisystems.com).

The measured potential of a test solution is converted into pH also using Eq. 1. In this case, if solution 1 is the test solution, then solution 2 is one of the standard solutions used for calibration.

The explicit equation for estimating the diffusion potential (also known as the isothermal liquid junction potential) is given by [10]

$$\Delta\phi_D = -\frac{RT}{F}\sum_i\int_A^B\frac{t_i}{z_i}d\ln a_i \tag{2}$$

where $t_i$ and $z_i$ refer, respectively, to the transport number and charge of the $i$th ionic species; and $A$ and $B$ represent two solutions across an isothermal junction. One of the most widely used approximations is based on the evaluation of the integral in Eq. 2 with the following simplifying conditions: (i) linear concentration gradient for each ionic species in the diffusion zone (that is, the junction is represented as a continuous series of mixtures with linearly varying proportions of the two solutions, A and B), (ii) constant mobilities for all species and (iii) the activity of each species is equal to its concentration. In addition, the transport number of ion $i$, $t_i$, is expressed either in terms of its mobility, $u_i$, or its conductivity, $\lambda_i = F\,u_i$, as

$$t_i = \frac{i_i}{i_t} = \frac{|z_i|m_iu_i}{\sum\limits_i|z_i|m_iu_i} = \frac{|z_i|m_i\lambda_i}{\sum\limits_i|z_i|m_i\lambda_i} \tag{3}$$

where $i_i$ is the current carried by ion $i$; $i_t$ is the total current, and $m_i$ is the molal concentration of ion $i$. The result is equivalent to the Henderson equation [10]

$$\Delta\phi_D = \phi_B - \phi_A = -\frac{RT}{F}\frac{\sum\limits_i\frac{\lambda_i|z_i|}{z_i}\left(m^B_i - m^A_i\right)}{\sum\limits_i\lambda_i|z_i|\left(m^B_i - m^A_i\right)}\ln\frac{\sum\limits_i\lambda_i|z_i|m^B_i}{\sum\limits_i\lambda_i|z_i|m^A_i} \tag{4}$$

where in Eq. 4, the limiting ionic conductivity, $\lambda^0_i$, is used instead of $\lambda_i$, for simplicity. Another approach for calculating the diffusion potentials was proposed by Harper [17]. This method retains the Henderson's continuous mixture assumption, but accounts for the nonideal behaviour of ions, namely for ionic mobilities and activities. Equation 2 then takes the following form

$$\Delta\phi_D = -\sum_i\frac{RT}{Fz_i}\int_0^1\frac{|z_i|\left\{\lambda^A_i + \left[\frac{\left[I^A+x\left(I^B-I^A\right)\right]^{1/3}-I^{A^{1/3}}}{I^{B^{1/3}}-I^{A^{1/3}}}\right]\left(\lambda^B_i - \lambda^A_i\right)\right\}}{\sum\limits_i|z_i|\left\{\lambda^A_i + \left[\frac{[I^A+x(I^B-I^A)]^{1/3}-I^{A^{1/3}}}{I^{B^{1/3}}-I^{A^{1/3}}}\right]\left(\lambda^B_i - \lambda^A_i\right)\right\}[m^A_i + x(m^B_i - m^A_i)]}$$
$$\left\{\left\{\left[\frac{\left(\ln\gamma^B_i - \ln\gamma^A_i\right)\left(I^B - I^A\right)}{\left(I^{B^{1/3}} - I^{A^{1/3}}\right)3\left[I^A + x\left(I^B - I^A\right)\right]^{2/3}}\right]\left[m^A_i + x\left(m^B_i - m^A_i\right)\right]\right\} + \left(m^B_i - m^A_i\right)\right\}dx \tag{5}$$

where $I$ is the ionic strength, $\gamma$ is the activity coefficient, and $x$ is the mixing fraction calculated by

$$m_i = m_i^A + x\left(m_i^B - m_i^A\right) \tag{6}$$

and having a value of 0 for pure solution $A$ and 1 for pure solution $B$. The ionic strength, $I$, is calculated by

$$I = \frac{1}{2}\sum_i z_i^2 m_i \tag{7}$$

Since both the Henderson equation, Eq. 4, and Harper's integral equation, Eq. 5, require knowledge of the concentrations of the component ions, the OLI Systems® software package was used, with a calibrated databank based on solubility measurements of Al, Mg and Ni in acidic sulphate solutions [18]. Ionic conductivities at infinite dilution were taken from the OLI's Public database, while those at finite concentration were taken from recent conductivity measurements in the $MgSO_4$–$H_2SO_4$–$H_2O$ system [19]. All other parameters required for Harper's equation (activity coefficients and ionic strengths of solutions) were determined within the OLI software. The integral in Eq. 5 was solved by numerical integration by using Maple V® software (Release 5, Student version, www.maplesoft.com). Numerical integration was performed by using the default Clenshaw–Curtis quadrature method [20].

## 4 Results and discussion

### 4.1 Effect of $MgSO_4$ on the pH of $H_2SO_{4(aq)}$ solutions at 250 °C with $NaCl_{(aq)}$ as the reference electrode solution

The experiments were carried out with the yttria-stabilized zirconia electrode denoted YSZ-1. Two sets of measurements were done, referred to as runs 1 and 2. The calibration data for electrode YSZ-1 at 250 °C, with NaCl as the reference solution, are given in Table 1. The calibration coefficient, α, was evaluated using Eq. 1, based on diffusion potentials calculated using either the Henderson equation or Harper's equation. The values of the calibration coefficient based on the diffusion potentials calculated using the Henderson equation are 0.951 and 0.935 for runs 1 and 2, respectively, while those based on the diffusion potentials evaluated using Harper's equation are 0.983 and 0.966 for runs 1 and 2, respectively.

Compositions of the test solutions and corresponding diffusion potentials are given in Table 2, while the experimental pH values based on the diffusion potentials calculated using the Henderson equation and Harper's equation are provided in Tables 3 and 4, respectively. The average differences between the theoretical and experimental pH values based on diffusion potentials calculated using either the Henderson or Harper's equation are the same, that is, 5.5% and 6.8% for 0.1 mol kg$^{-1}$ $H_2SO_4$ and 0.3 mol kg$^{-1}$ $H_2SO_4$, respectively, or 6.1% on average.

**Table 1** The calibration data for $MgSO_4$–$H_2SO_4$–$H_2O$ and $NiSO_4$–$H_2SO_4$–$H_2O$ systems at 250 °C

| Calibration solution | Measured potentials (mV) | | $\Delta\phi_D$ (mV) | | pH (OLI) |
|---|---|---|---|---|---|
| | YSZ-1 run 1 | YSZ-1 run 2 | Henderson | Harper | |
| 0.005 mol kg$^{-1}$ $H_2SO_4$ | 624 | 625 | −18.1 | −15.9 | 2.36 |
| 0.01 mol kg$^{-1}$ $H_2SO_4$ | 665 | 648 | −17.4 | −15.1 | 2.08 |
| 0.02 mol kg$^{-1}$ $H_2SO_4$ | 676 | 678 | −18.0 | −15.4 | 1.81 |
| 0.05 mol kg$^{-1}$ $H_2SO_4$ | 723 | 719 | −21.2 | −17.8 | 1.47 |
| 0.1 mol kg$^{-1}$ $H_2SO_4$ | 738 | 746 | −25.7 | −21.3 | 1.21 |
| 0.3 mol kg$^{-1}$ $H_2SO_4$ | 775 | 769 | −36.6 | −29.5 | 0.82 |

The diffusion potentials ($\Delta\phi_D$) are calculated using either the Henderson or Harper's equation. The reference electrode solution is 0.1 mol kg$^{-1}$ NaCl

It can be seen (Tables 1, 2) that the diffusion potentials calculated using the Henderson equation were higher by as much as 7.1 mV than those evaluated using Harper's equation (in the negative direction). The main reason is that the Henderson equation includes limiting ionic conductivities, which makes the hydrogen ion more mobile than in concentrated multi-component solutions. Nevertheless, experimental pH values calculated using diffusion potentials evaluated by either approach are similar, as it can be seen from Tables 3 and 4. This finding suggests that these differences are accounted for during the calibration procedure and that the calculation of pH can be based on the diffusion potentials evaluated using the Henderson equation. It is an important conclusion because the ionic conductivities at finite concentrations are not usually available to employ the more accurate Harper's equation. Consequently, the calculation of pH in all experiments reported in this paper was based on the diffusion potentials evaluated using the Henderson equation, Eq. 4.

The experimental pH values based on diffusion potentials calculated using the Henderson equation are also illustrated in Fig. 2. It is obvious that increasing $MgSO_4$ concentration results in an increase in pH. Seneviratne et al. [4] also found that pH increases with increasing $MgSO_4$ levels in the $MgSO_4$–$Al_2(SO_4)_3$–$H_2SO_4$–$H_2O$ system. These findings also agree well with those of Baghalha and Papangelakis [5], who found by calculation that increasing $MgSO_4$ levels caused a sharp drop in hydrogen ion molality. This behaviour was attributed to the dissociation of $MgSO_4$, where the $SO_4^{2-}$(aq) introduced to a test solution reacted with $H^+$(aq) to form $HSO_4^-$(aq) [5]. These observations are also consistent with those in the industrial practice of pressure acid

**Table 2** The composition of test solutions and corresponding diffusion potentials for the $MgSO_4$–$H_2SO_4$–$H_2O$ system at 250 °C

The diffusion potentials ($\Delta\phi_D$) are calculated using either the Henderson or Harper's equation. The reference electrode solution is 0.1 mol kg$^{-1}$ NaCl

| Test solution | Solution composition | $\Delta\phi_D$ (mV) | |
|---|---|---|---|
| | | Henderson | Harper |
| Mg1 | 0.1 mol kg$^{-1}$ $H_2SO_4$ + 0.01 mol kg$^{-1}$ $MgSO_4$ | −21.4 | −16.5 |
| Mg2 | 0.1 mol kg$^{-1}$ $H_2SO_4$ + 0.04 mol kg$^{-1}$ $MgSO_4$ | −8.5 | −3.5 |
| Mg3 | 0.1 mol kg$^{-1}$ $H_2SO_4$ + 0.07 mol kg$^{-1}$ $MgSO_4$ | 4.2 | 6.5 |
| Mg6 | 0.3 mol kg$^{-1}$ $H_2SO_4$ + 0.05 mol kg$^{-1}$ $MgSO_4$ | −25.1 | −18.0 |
| Mg7 | 0.3 mol kg$^{-1}$ $H_2SO_4$ + 0.1 mol kg$^{-1}$ $MgSO_4$ | −13.5 | −6.4 |
| Mg8 | 0.3 mol kg$^{-1}$ $H_2SO_4$ + 0.15 mol kg$^{-1}$ $MgSO_4$ | −2.0 | 4.6 |

**Table 3** The comparison between experimental pH values and theoretical pH values (OLI) for the $MgSO_4$–$H_2SO_4$–$H_2O$ system at 250 °C

The experimental pH is calculated based on diffusion potentials evaluated using the Henderson equation. The reference electrode solution is 0.1 mol kg$^{-1}$ NaCl

| Test solution | Measured values | | | | Average measured pH | Standard deviation | pH (OLI) |
|---|---|---|---|---|---|---|---|
| | YSZ-1 run 1 | | YSZ-1 run 2 | | | | |
| | E (mV) | pH | E (mV) | pH | | | |
| Mg1 | 748 | 1.20 | 754 | 1.13 | 1.17 | 0.049 | 1.27 |
| Mg2 | 739 | 1.40 | 728 | 1.49 | 1.45 | 0.064 | 1.48 |
| Mg3 | 706 | 1.83 | 692 | 1.94 | 1.89 | 0.078 | 1.78 |
| Mg6 | 783 | 0.84 | 775 | 0.91 | 0.88 | 0.049 | 0.92 |
| Mg7 | 768 | 1.09 | 761 | 1.15 | 1.12 | 0.042 | 1.04 |
| Mg8 | 753 | 1.34 | 765 | 1.22 | 1.28 | 0.085 | 1.17 |

**Table 4** The comparison between experimental pH values and theoretical pH values (OLI) for the $MgSO_4$–$H_2SO_4$–$H_2O$ system at 250 °C

The experimental pH is calculated based on diffusion potentials evaluated using Harper's equation. The reference electrode solution is 0.1 mol kg$^{-1}$ NaCl

| Test solution | Measured values | | | | Average measured pH | Standard deviation | pH (OLI) |
|---|---|---|---|---|---|---|---|
| | YSZ-1 run 1 | | YSZ-1 run 2 | | | | |
| | E (mV) | pH | E (mV) | pH | | | |
| Mg1 | 748 | 1.19 | 754 | 1.12 | 1.16 | 0.049 | 1.27 |
| Mg2 | 739 | 1.40 | 728 | 1.48 | 1.44 | 0.057 | 1.48 |
| Mg3 | 706 | 1.81 | 692 | 1.90 | 1.86 | 0.064 | 1.78 |
| Mg6 | 783 | 0.85 | 775 | 0.92 | 0.89 | 0.049 | 0.92 |
| Mg7 | 768 | 1.10 | 761 | 1.16 | 1.13 | 0.042 | 1.04 |
| Mg8 | 753 | 1.35 | 765 | 1.23 | 1.29 | 0.085 | 1.17 |

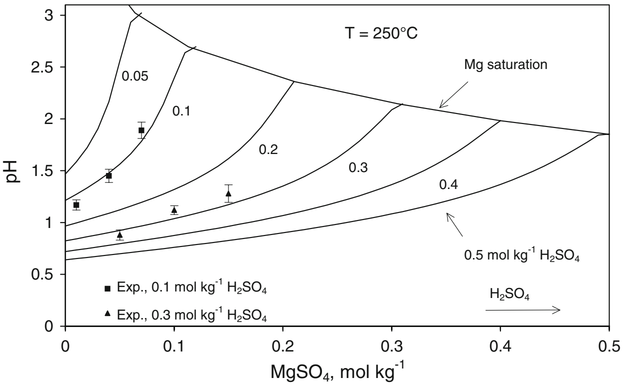

**Fig. 2** Theoretical pH (lines) versus $MgSO_4$ concentration at different $H_2SO_4$ concentrations. The experimental pH values at 0.1 mol kg$^{-1}$ $H_2SO_4$ and 0.3 mol kg$^{-1}$ $H_2SO_4$ are shown as squares and triangles, respectively. The reference electrode solution is 0.1 mol kg$^{-1}$ NaCl. The diffusion potentials are calculated using the Henderson equation

leaching of high-magnesium laterite ores, which are known for their elevated acid consumption [1].

## 4.2 Effect of $NiSO_4$ on the pH of $H_2SO_{4(aq)}$ solutions at 250 °C with $NaCl_{(aq)}$ as the reference electrode solution

Yttria-stabilized zirconia electrode YSZ-1 was used in these experiments. Two sets of measurements were done, namely runs 1 and 2. Compositions of the test solutions and corresponding diffusion potentials are shown in Table 5. The experimental pH values, based on the diffusion potentials calculated using the Henderson equation, are depicted in Fig. 3. The average difference between the theoretical and experimental pH values is 2.1% and 5.8% at 0.1 mol kg$^{-1}$ $H_2SO_4$ and 0.3 mol kg$^{-1}$ $H_2SO_4$, respectively, or 3.9% on average. It can be seen that nickel sulphate behaves similarly to magnesium sulphate. This

**Table 5** The composition of test solutions and corresponding diffusion potentials for the $NiSO_4$–$H_2SO_4$–$H_2O$ system at 250 °C

| Test Solution | Solution composition | $\Delta\phi_D$ (mV) |
|---|---|---|
| Ni1 | 0.1 mol $kg^{-1}$ $H_2SO_4$ + 0.01 mol $kg^{-1}$ $NiSO_4$ | −21.4 |
| Ni2 | 0.1 mol $kg^{-1}$ $H_2SO_4$ + 0.04 mol $kg^{-1}$ $NiSO_4$ | −8.3 |
| Ni3 | 0.1 mol $kg^{-1}$ $H_2SO_4$ + 0.07 mol $kg^{-1}$ $NiSO_4$ | 4.7 |
| Ni4 | 0.3 mol $kg^{-1}$ $H_2SO_4$ + 0.05 mol $kg^{-1}$ $NiSO_4$ | −25.0 |
| Ni5 | 0.3 mol $kg^{-1}$ $H_2SO_4$ + 0.1 mol $kg^{-1}$ $NiSO_4$ | −13.3 |
| Ni6 | 0.3 mol $kg^{-1}$ $H_2SO_4$ + 0.15 mol $kg^{-1}$ $NiSO_4$ | −1.7 |

The diffusion potentials ($\Delta\phi_D$) are calculated using the Henderson equation. The reference electrode solution is 0.1 mol $kg^{-1}$ NaCl

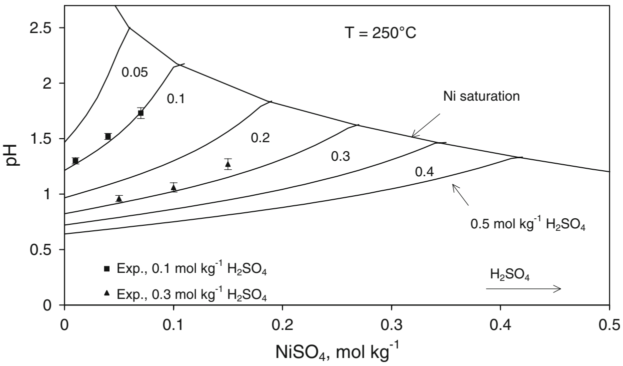

**Fig. 3** Theoretical pH (lines) versus $NiSO_4$ concentration at different $H_2SO_4$ concentrations. The experimental pH values at 0.1 mol $kg^{-1}$ $H_2SO_4$ and 0.3 mol $kg^{-1}$ $H_2SO_4$ are shown as squares and triangles, respectively. The reference electrode solution is 0.1 mol $kg^{-1}$ NaCl

observation is supported by the results of the studies on the solubilities of $NiSO_4$ and $MgSO_4$ in $H_2SO_4$ solutions [18].

## 4.3 Effect of $MgSO_4$ on the pH of $H_2SO_{4(aq)}$ solutions at 200 °C with $NaCl_{(aq)}$ as the reference electrode solution

The experiments were performed with the electrode denoted YSZ-2. Two sets of measurements were done, namely runs 1 and 2. The calibration data for electrode YSZ-2 at 200 °C, with NaCl as the reference electrode solution, are provided in Table 6. The values of the calibration coefficient are 0.886 and 0.840 for runs 1 and 2, respectively.

Compositions of the test solutions and corresponding diffusion potentials are given in Table 7. The experimental pH values, based on the diffusion potentials calculated using the Henderson equation, are shown in Fig. 4. The average difference between the theoretical and experimental pH values is 3.8% and 3.5% for 0.1 mol $kg^{-1}$ $H_2SO_4$ and 0.3 mol $kg^{-1}$ $H_2SO_4$, respectively, or 3.7% on average. It is evident that increasing $MgSO_4$ concentration leads to an increase in pH, as was the case at 250 °C. By comparing Figs. 2 and 4, it can also be seen that increasing temperature from 200 °C to 250 °C results in a decrease of pH, which can be attributed to a decrease of the dielectric constant of water when temperature is increasing.

## 4.4 Effect of $MgSO_4$ on the pH of $H_2SO_{4(aq)}$ solutions at 250 °C and 200 °C with $LiCl_{(aq)}$ as the reference electrode solution

As already mentioned in this paper, scale formation at the outlet of the electrochemical cell was observed during measurements of pH in PAL solutions. The scale was produced because of mixing of the aluminium-containing PAL solutions and the NaCl reference electrode solution. The precipitation of sodium alunite forced us to investigate whether sodium chloride can be replaced with another chloride salt having a cation that does not produce an alunite type of compound and would not induce scaling in the electrochemical cell. Lithium chloride was selected because it is well established that lithium does not form jarosite-type compounds [21]. Alunite and jarosite (the

**Table 6** The calibration data for the $MgSO_4$–$H_2SO_4$–$H_2O$ system at 200 °C

| Calibration solution | Measured potentials (mV) | | $\Delta\phi_D$ (mV) | pH (OLI) |
|---|---|---|---|---|
| | YSZ-2 run 1 | YSZ-2 run 2 | | |
| 0.005 mol $kg^{-1}$ $H_2SO_4$ | 584 | 578 | −18.4 | 2.35 |
| 0.01 mol $kg^{-1}$ $H_2SO_4$ | 617 | 605 | −18.0 | 2.07 |
| 0.02 mol $kg^{-1}$ $H_2SO_4$ | 635 | 641 | −19.0 | 1.79 |
| 0.05 mol $kg^{-1}$ $H_2SO_4$ | 663 | 660 | −23.0 | 1.43 |
| 0.1 mol $kg^{-1}$ $H_2SO_4$ | 703 | 688 | −28.3 | 1.17 |
| 0.3 mol $kg^{-1}$ $H_2SO_4$ | 728 | 736 | −40.4 | 0.75 |

The diffusion potentials ($\Delta\phi_D$) are calculated using the Henderson equation. The reference electrode solution is 0.1 mol $kg^{-1}$ NaCl

**Table 7** The composition of test solutions and corresponding diffusion potentials for the $MgSO_4$–$H_2SO_4$–$H_2O$ system at 200 °C

| Test solution | Solution composition | $\Delta\phi_D$ (mV) |
|---|---|---|
| Mg1 | 0.1 mol $kg^{-1}$ $H_2SO_4$ + 0.01 mol $kg^{-1}$ $MgSO_4$ | −24.3 |
| Mg2 | 0.1 mol $kg^{-1}$ $H_2SO_4$ + 0.04 mol $kg^{-1}$ $MgSO_4$ | −12.0 |
| Mg3 | 0.1 mol $kg^{-1}$ $H_2SO_4$ + 0.07 mol $kg^{-1}$ $MgSO_4$ | 0.4 |
| Mg4 | 0.1 mol $kg^{-1}$ $H_2SO_4$ + 0.09 mol $kg^{-1}$ $MgSO_4$ | 7.5 |
| Mg5 | 0.1 mol $kg^{-1}$ $H_2SO_4$ + 0.11 mol $kg^{-1}$ $MgSO_4$ | 10.9 |
| Mg6 | 0.3 mol $kg^{-1}$ $H_2SO_4$ + 0.05 mol $kg^{-1}$ $MgSO_4$ | −29.8 |
| Mg7 | 0.3 mol $kg^{-1}$ $H_2SO_4$ + 0.1 mol $kg^{-1}$ $MgSO_4$ | −18.8 |
| Mg9 | 0.3 mol $kg^{-1}$ $H_2SO_4$ + 0.2 mol $kg^{-1}$ $MgSO_4$ | 3.4 |

The diffusion potentials ($\Delta\phi_D$) are calculated using the Henderson equation. The reference electrode solution is 0.1 mol $kg^{-1}$ NaCl

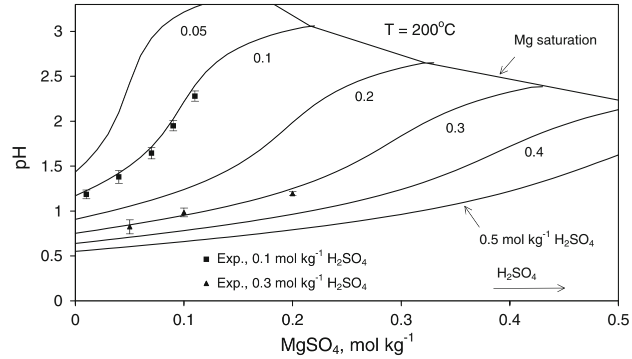

**Fig. 4** Theoretical pH (lines) versus $MgSO_4$ concentration at different $H_2SO_4$ concentrations. The experimental pH values at 0.1 mol $kg^{-1}$ $H_2SO_4$ and 0.3 mol $kg^{-1}$ $H_2SO_4$ are shown as squares and triangles, respectively. The reference electrode solution is 0.1 mol $kg^{-1}$ NaCl

**Table 8** The calibration data for $MgSO_4$–$H_2SO_4$–$H_2O$ and $NiSO_4$–$H_2SO_4$–$H_2O$ systems at 250 °C

| Calibration solution | Measured potentials (mV) | | $\Delta\phi_D$ (mV) | pH (OLI) |
|---|---|---|---|---|
| | YSZ-1 run 3 | YSZ-1 run 4 | | |
| 0.005 mol $kg^{-1}$ $H_2SO_4$ | 619 | 613 | −24.9 | 2.36 |
| 0.01 mol $kg^{-1}$ $H_2SO_4$ | 644 | 653 | −22.9 | 2.08 |
| 0.02 mol $kg^{-1}$ $H_2SO_4$ | 665 | 681 | −22.3 | 1.81 |
| 0.05 mol $kg^{-1}$ $H_2SO_4$ | 704 | 711 | −24.3 | 1.47 |
| 0.1 mol $kg^{-1}$ $H_2SO_4$ | 729 | 724 | −28.1 | 1.21 |
| 0.3 mol $kg^{-1}$ $H_2SO_4$ | 751 | 763 | −38.2 | 0.82 |

The diffusion potentials ($\Delta\phi_D$) are calculated using the Henderson equation. The reference electrode solution is 0.1 mol $kg^{-1}$ LiCl

Fe(III) equivalent) are isomorphic compounds, and therefore it is natural to expect some similarity in their chemical properties.

Thus, the pH of the ternary $MgSO_4$–$H_2SO_4$–$H_2O$ system was measured at temperatures of 250 °C and 200 °C with 0.1 mol $kg^{-1}$ LiCl as the reference electrode solution. The yttria-stabilized zirconia electrode denoted YSZ-1 was used at 250 °C, while the electrode denoted YSZ-2 was used at 200 °C. Two sets of measurements were done with each YSZ electrode, referred to as runs 3 and 4. The calibration data for electrodes YSZ-1 at 250 °C and YSZ-2 at 200 °C are given in Tables 8 and 9, respectively. For electrode YSZ-1, the values of the calibration coefficient are 1.073 and 1.030 for runs 3 and 4, respectively. For electrode YSZ-2, the values of the calibration coefficient are 0.897 and 0.932 for runs 3 and 4, respectively.

The test solutions compositions and the corresponding diffusion potentials are provided in Tables 10 and 11. Experimental pH values are shown in Figs. 5 and 6. As expected, solution pH increases with increasing $MgSO_4$ levels, as was the case in the $MgSO_4$–$H_2SO_4$–$H_2O$ systems with 0.1 mol $kg^{-1}$ NaCl as the reference electrode solution. At 250 °C, the average difference between the theoretical and the experimental pH values is 4.7% and 3.5% at 0.1 mol $kg^{-1}$ $H_2SO_{4(aq)}$ and 0.3 mol $kg^{-1}$ $H_2SO_{4(aq)}$, respectively, or 4.1% on average, whereas, at 200 °C, the average difference between the theoretical and the experimental pH values is 4.6% and 5.5% at 0.1 m $H_2SO_4$ and 0.3 m $H_2SO_4$, respectively, or 4.9% on average. Therefore, it can be concluded that $LiCl_{(aq)}$ is a suitable alternative to $NaCl_{(aq)}$ to be used as the reference electrode solution.

## 4.5 Effect of $NiSO_4$ on the pH of $H_2SO_{4(aq)}$ solutions at 250 °C with $LiCl_{(aq)}$ as the reference electrode solution

Yttria-stabilized zirconia electrode YSZ-1 was used in these experiments. Two sets of measurements were done, namely runs 3 and 4. Compositions of the test solutions and corresponding diffusion potentials are given in Table 12. Experimental pH values are depicted in Fig. 7. It is evident that solution pH increases with increasing $NiSO_4$ concentration, as was the case in the $NiSO_4$–$H_2SO_4$–$H_2O$ system with $NaCl_{(aq)}$ as the reference electrode solution. The average difference between the theoretical and the experimental pH values is 4.0% and 5.4% at 0.1 mol $kg^{-1}$ $H_2SO_4$ and 0.3 mol $kg^{-1}$ $H_2SO_4$, respectively, or 4.7% on average. Again, it can be seen that $LiCl_{(aq)}$ provides essentially the same level of accuracy as $NaCl_{(aq)}$ does.

**Table 9** The calibration data for the $MgSO_4$–$H_2SO_4$–$H_2O$ system at 200 °C

| Calibration solution | Measured potentials (mV) | | $\Delta\phi_D$ (mV) | pH (OLI) |
|---|---|---|---|---|
| | YSZ-2 run 3 | YSZ-2 run 4 | | |
| 0.005 mol $kg^{-1}$ $H_2SO_4$ | 579 | 574 | −25.4 | 2.35 |
| 0.01 mol $kg^{-1}$ $H_2SO_4$ | 603 | 595 | −23.6 | 2.07 |
| 0.02 mol $kg^{-1}$ $H_2SO_4$ | 640 | 633 | −23.4 | 1.79 |
| 0.05 mol $kg^{-1}$ $H_2SO_4$ | 653 | 660 | −26.2 | 1.43 |
| 0.1 mol $kg^{-1}$ $H_2SO_4$ | 685 | 692 | −30.7 | 1.17 |
| 0.3 mol $kg^{-1}$ $H_2SO_4$ | 726 | 718 | −42.2 | 0.75 |

The diffusion potentials ($\Delta\phi_D$) are calculated using the Henderson equation. The reference electrode solution is 0.1 mol $kg^{-1}$ LiCl

**Table 10** The composition of test solutions and corresponding diffusion potentials for the $MgSO_4$–$H_2SO_4$–$H_2O$ system at 250 °C

| Test solution | Solution composition | $\Delta\phi_D$ (mV) |
|---|---|---|
| Mg1 | 0.1 mol $kg^{-1}$ $H_2SO_4$ + 0.01 mol $kg^{-1}$ $MgSO_4$ | −23.7 |
| Mg2 | 0.1 mol $kg^{-1}$ $H_2SO_4$ + 0.04 mol $kg^{-1}$ $MgSO_4$ | −10.5 |
| Mg3 | 0.1 mol $kg^{-1}$ $H_2SO_4$ + 0.07 mol $kg^{-1}$ $MgSO_4$ | 2.4 |
| Mg6 | 0.3 mol $kg^{-1}$ $H_2SO_4$ + 0.05 mol $kg^{-1}$ $MgSO_4$ | −26.5 |
| Mg7 | 0.3 mol $kg^{-1}$ $H_2SO_4$ + 0.1 mol $kg^{-1}$ $MgSO_4$ | −14.7 |
| Mg8 | 0.3 mol $kg^{-1}$ $H_2SO_4$ + 0.15 mol $kg^{-1}$ $MgSO_4$ | −3.0 |

The diffusion potentials ($\Delta\phi_D$) are calculated using the Henderson equation. The reference electrode solution is 0.1 mol $kg^{-1}$ LiCl

**Table 11** The composition of test solutions and corresponding diffusion potentials for the $MgSO_4$–$H_2SO_4$–$H_2O$ system at 200 °C

| Test solution | Solution composition | $\Delta\phi_D$ (mV) |
|---|---|---|
| Mg1 | 0.1 mol $kg^{-1}$ $H_2SO_4$ + 0.01 mol $kg^{-1}$ $MgSO_4$ | −26.6 |
| Mg2 | 0.1 mol $kg^{-1}$ $H_2SO_4$ + 0.04 mol $kg^{-1}$ $MgSO_4$ | −14.1 |
| Mg3 | 0.1 mol $kg^{-1}$ $H_2SO_4$ + 0.07 mol $kg^{-1}$ $MgSO_4$ | −1.5 |
| Mg4 | 0.1 mol $kg^{-1}$ $H_2SO_4$ + 0.09 mol $kg^{-1}$ $MgSO_4$ | 5.8 |
| Mg5 | 0.1 mol $kg^{-1}$ $H_2SO_4$ + 0.11 mol $kg^{-1}$ $MgSO_4$ | 9.3 |
| Mg6 | 0.3 mol $kg^{-1}$ $H_2SO_4$ + 0.05 mol $kg^{-1}$ $MgSO_4$ | −31.3 |
| Mg7 | 0.3 mol $kg^{-1}$ $H_2SO_4$ + 0.1 mol $kg^{-1}$ $MgSO_4$ | −20.2 |
| Mg9 | 0.3 mol $kg^{-1}$ $H_2SO_4$ + 0.2 mol $kg^{-1}$ $MgSO_4$ | 2.5 |

The diffusion potentials ($\Delta\phi_D$) are calculated using the Henderson equation. The reference electrode solution is 0.1 mol $kg^{-1}$ LiCl

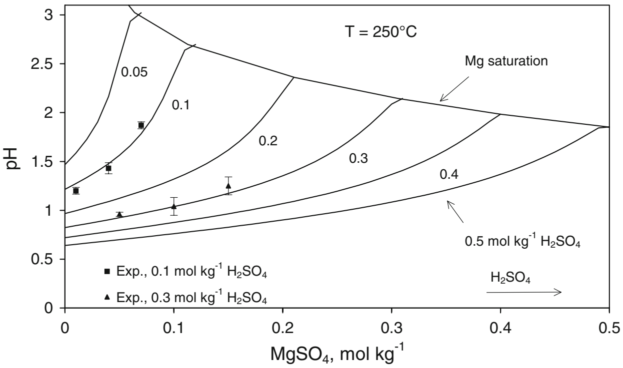

**Fig. 5** Theoretical pH (lines) versus $MgSO_4$ concentration at different $H_2SO_4$ concentrations. The experimental pH values at 0.1 mol $kg^{-1}$ $H_2SO_4$ and 0.3 mol $kg^{-1}$ $H_2SO_4$ are shown as squares and triangles, respectively. The reference electrode solution is 0.1 mol $kg^{-1}$ LiCl

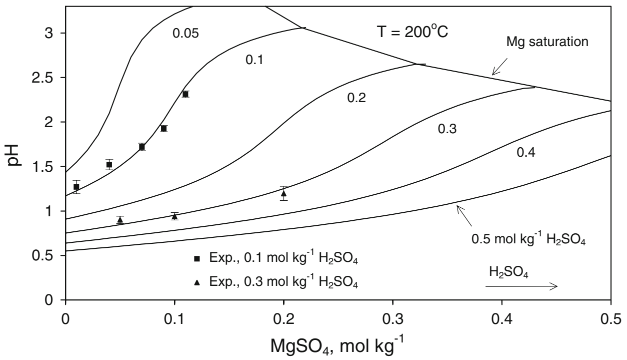

**Fig. 6** Theoretical pH (lines) versus $MgSO_4$ concentration at different $H_2SO_4$ concentrations. The experimental pH values at 0.1 mol $kg^{-1}$ $H_2SO_4$ and 0.3 mol $kg^{-1}$ $H_2SO_4$ are shown as squares and triangles, respectively. The reference electrode solution is 0.1 mol $kg^{-1}$ LiCl

## 5 Conclusions

A flow-through potentiometric technique utilizing an yttria-stabilized zirconia (YSZ) pH sensor was employed to elucidate the effects of nickel sulphate and magnesium sulphate on pH of sulphuric acid solutions at temperatures of 200 °C and 250 °C. The pH of sulphuric acid solutions was found to increase with increasing magnesium sulphate

**Table 12** The composition of test solutions and corresponding diffusion potentials for the $NiSO_4$–$H_2SO_4$–$H_2O$ system at 250 °C

| Test solution | Solution composition | $\Delta\phi_D$ (mV) |
|---|---|---|
| Ni1 | 0.1 mol $kg^{-1}$ $H_2SO_4$ + 0.01 mol $kg^{-1}$ $NiSO_4$ | −23.7 |
| Ni2 | 0.1 mol $kg^{-1}$ $H_2SO_4$ + 0.04 mol $kg^{-1}$ $NiSO_4$ | −10.3 |
| Ni3 | 0.1 mol $kg^{-1}$ $H_2SO_4$ + 0.07 mol $kg^{-1}$ $NiSO_4$ | −3.0 |
| Ni6 | 0.3 mol $kg^{-1}$ $H_2SO_4$ + 0.05 mol $kg^{-1}$ $NiSO_4$ | −26.4 |
| Ni7 | 0.3 mol $kg^{-1}$ $H_2SO_4$ + 0.1 mol $kg^{-1}$ $NiSO_4$ | −14.6 |
| Ni8 | 0.3 mol $kg^{-1}$ $H_2SO_4$ + 0.15 mol $kg^{-1}$ $NiSO_4$ | −2.7 |

The diffusion potentials ($\Delta\phi_D$) are calculated using the Henderson equation. The reference electrode solution is 0.1 mol $kg^{-1}$ LiCl

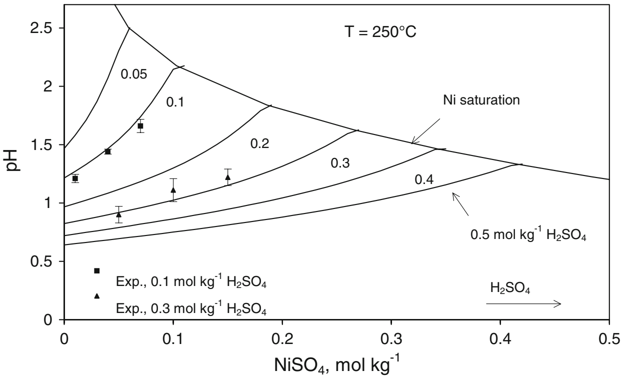

**Fig. 7** Theoretical pH (lines) versus $NiSO_4$ concentration at different $H_2SO_4$ concentrations. The experimental pH values at 0.1 mol $kg^{-1}$ $H_2SO_4$ and 0.3 mol $kg^{-1}$ $H_2SO_4$ are shown as squares and triangles, respectively. The reference electrode solution is 0.1 mol $kg^{-1}$ LiCl

and nickel sulphate concentrations at both 200 °C and 250 °C. This trend is attributed to the dissociation of $MgSO_4$ and $NiSO_4$ where the $SO_4^{2-}$(aq) is released and reacts with $H^+$(aq) to form $HSO_4^-$(aq). Furthermore, increasing temperature from 200 °C to 250 °C resulted in a decrease of pH, which can be attributed to a decrease of the dielectric constant of water when temperature is increasing. Conversion of the measured potentials into pH values was based on the mixed-solvent electrolyte (MSE) model using the new OLI Systems® software. In addition, a simple Henderson equation was effectively used to calculate the diffusion potentials. Finally, lithium chloride was found to be a suitable alternative to sodium chloride as the reference electrode solution.

**Acknowledgments** We would like to acknowledge the financial support provided by the Natural Sciences and Engineering Research Council of Canada (NSERC). We are grateful to Dr. Haixia Liu for providing speciation calculations. We would also like to thank Dr. David Wesolowski, Prof. William Seyfried, Jr., and Prof. Kwadwo Osseo-Asare for providing reviews of an earlier version of this paper.

## References

1. Baghalha M, Papangelakis VG (1998) Metall Mater Trans 29B:945
2. Krause E, Singhal A, Blakey BC et al (1997) In: Cooper WC, Mihaylov I (eds) Nickel–Cobalt 97 international symposium vol I. The Canadian Institute of Mining, Metallurgy and Petroleum, Montreal, Canada, pp 441–458
3. Rubisov DH, Papangelakis VG (2000) Hydrometallurgy 58:13
4. Seneviratne DS, Papangelakis VG, Zhou XY, Lvov SN (2003) Hydrometallurgy 68:131
5. Baghalha M, Papangelakis VG (1998) Metall Mater Trans 29B:1021
6. Ridley MK, Wesolowski DJ, Palmer DA, Kettler RM (1999) Geochim Cosmochim Acta 63:459
7. Tagirov B, Schott J (2001) Geochim Cosmochim Acta 65:3965
8. Lvov SN, Gao H, Kouznetsov D et al (1998) Fluid Phase Equilibria 150–151:515
9. Lvov SN, Zhou XY, Ulyanov SM et al (2004) In: Collins MJ, Papangelakis VG (eds) Pressure hydrometallurgy 2004. The Canadian Institute of Mining, Metallurgy and Petroleum, Banff, Canada, pp 561–576
10. MacInnes DA (1961) The principles of electrochemistry. Dover Publications, New York, pp 220–232
11. Lvov SN, Palmer DA (2004) In: Palmer DA, Fernandez-Prini R, Harvey AH (eds) Aqueous systems at elevated temperatures and pressures: Physical chemistry in water, steam and hydrothermal solutions. Elsevier Academic Press, Amsterdam, pp 377–408
12. Lvov SN, Zhou XY, Ulmer GC et al (2003) Chem Geol 198:141
13. Lvov SN (2007) In: Bard AJ, Stratmann M, Macdonald DD, Schmuki P (eds) Encyclopedia of electrochemistry, vol 5. Wiley-VCH, Weinheim, pp 723–747
14. Lvov SN, Gao H, Macdonald DD (1998) J Electroanal Chem 443:186
15. Macdonald DD, Hettiarachchi S, Lenhart SJ (1988) J Solution Chem 17:719
16. Lvov SN, Zhou XY, Macdonald DD (1999) J Electroanal Chem 463:146
17. Harper HW (1985) J Phys Chem 89:1659
18. Liu H, Papangelakis VG (2005) Hydrometallurgy 79:48
19. Huang M, Papangelakis VG (2006) Ind Eng Chem Res 45:4757
20. Heck A (1996) Introduction to maple, 2nd edn. Springer-Verlag, New York, pp 241–242
21. Dutrizac JE, Jambor JL (1987) Hydrometallurgy 17:251